TRANSPORTATION RESEARCH RECORD 1526: Emerging Technologies in Geotechnical Engineering. National Academy Press, washington, DC. 1996

Digital-Image-Based Computer Modeling and Visualization of Cement-Based Materials

DALE P. BENTZ AND EDWARD J. GARBOCZI

Over the past several years, digital-image-based computer models and subsequent visualization of microstructure have proven valuable in studying processing-microstructure-property relationships in cement-based materials. This paper reviews the computer modeling techniques used to simulate the microstructure of hydrating cement paste at the micrometer level and the microstructure of concrete and mortar at the millimeter level. In the former case, digital-image-based models using cellular automata offer many advantages in simulating the reactions occurring during the hydration of cement paste. In the latter case, a continuum hard core–soft shell percolation model appears to be most efficient for modeling the aggregates in a mortar or concrete, each surrounded by an interfacial transition zone (ITZ). Here, digitization is employed to compute the volume fractions occupied by aggregate, bulk cement paste, and ITZ cement paste. The influence of microstructure on the diffusivity of these materials is addressed within the overall framework of this multiscale modeling approach.

In any effort to improve the performance of materials, a basic understanding of the relationships between microstructure and properties can be of great value. In the case of cement-based materials, the inherent complexities of the microstructure have provided the impetus for the application of computer modeling techniques to extract key microstructure-property relationships (*1*). By representing the microstructure as a digital image in two or three dimensions, microstructural evolution and property computations can be performed in a straightforward manner, the former employing cellular automata (*2,3*) techniques and the latter using a mapping onto a finite difference (*4*) or finite element (*5*) grid.

A limitation of the digital-image-based approach for cement-based materials is one of resolution. For example, in a simulation where each pixel represents 1 μm^3 in volume, it is difficult to perform a simulation containing aggregates several centimeters in diameter and cement particles some 10 μm in diameter, even with recent advances in computer memory and speed. Recently, this limitation has been overcome by applying a multiscale approach to the simulation of microstructure and properties (*6,7*). Here, separate microstructure models are developed at each scale of interest and then linked together to provide a flow of information from one scale to the next. For example, concrete or mortar can be modeled on the millimeter scale as a three-phase composite consisting of aggregates surrounded by regions of interfacial transition zone (ITZ) cement paste, with the remainder of the volume being occupied by the bulk cement paste. Appropriate properties for the bulk and ITZ cement paste can be determined from a micrometer-level model of the cement paste consisting of unhydrated cement particles, capillary porosity, and crystalline and gel hydration products. Similarly, appropriate properties for the gel hydration products could be determined from a nanometer level model of the gel structure (*6*).

In this paper, modeling of the diffusivity of a mortar or concrete will be described. To do this, a linkage is developed between a digital-image-based microstructure model for cement hydration at the micrometer level (*3,8*) and a continuum-based hard core–soft shell spherical inclusion microstructure model for concrete and mortar at the millimeter level (*9,10*).

National Institute of Standards and Technology, Building and Fire Research Laboratory, Building 226, Room B-350, Gaithersburg, Md. 20899-0001.

COMPUTER MODELING TECHNIQUES

Microstructure Model for Hydrating Cement Paste

Initial work on digital-image-based models for cement hydration focused on a model for the hydration of tricalcium silicate (C_3S) (*8*), the major component of most portland cements. More recently, the model has been extended to account for all of the major phases present in an ordinary portland cement (*3*). In the extended model, a combination of scanning electron microscope backscattered electron and X-ray images can be processed to obtain an image of the starting cement paste in which each pixel in the digital image has been assigned its appropriate mineralogical phase (*11*). Figure 1 shows a series of such images obtained for four different portland cements, illustrating the variety of phase distributions possible in these complex materials. In these images, the phases from brightest to darkest are tricalcium aluminate, gypsum, tetracalcium aluminoferrite, tricalcium silicate, dicalcium silicate, and capillary porosity. Accounting for this phase and size variation is critical for correlating the model predictions and experimental performance of a given cement.

For both the C_3S and multiphase cement microstructure models, cellular automata are used to simulate the hydration process over time (*3*). The model provides rules for the dissolution of the original cement minerals, diffusion of species within the available water-filled pore space, and nucleation and precipitation of hydration products. Throughout the simulation, the appropriate volume stoichiometry is maintained, as the hydration products occupy a greater volume than the initial cement, transforming the cement paste from a viscous suspension into a rigid load-bearing solid. By applying these rules to initial starting images like those shown in Figure 1, the microstructure at any given time (degree of hydration) can be modeled and used as input into property-computation algorithms. The degree of hydration is monitored by computing the fraction of the initial cement that remains unhydrated as the model evolves.

Figure 2 illustrates the basic steps in the C_3S hydration model. In this figure, unhydrated C_3S is white, calcium hydroxide is light

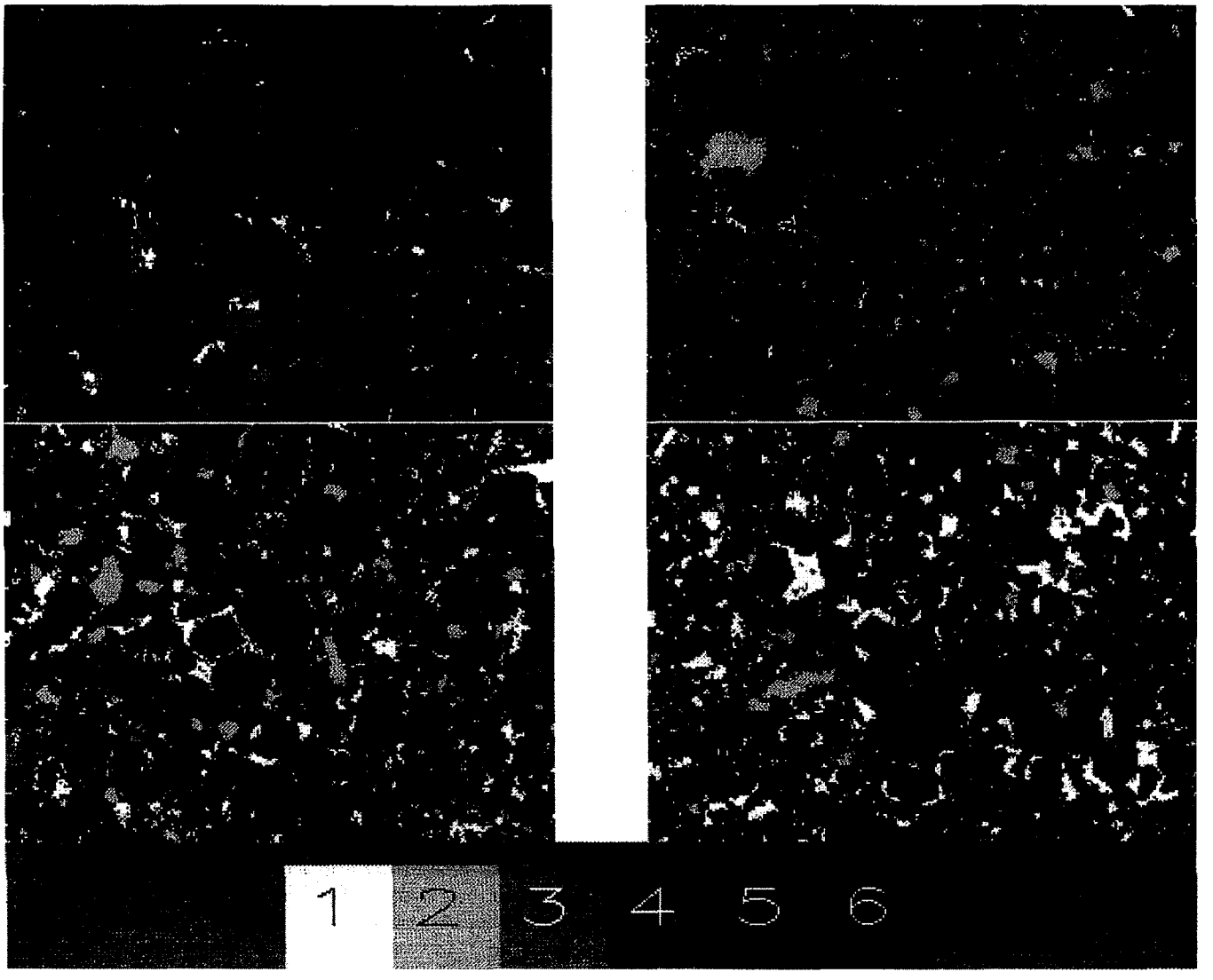

FIGURE 1 Starting images for four different portland cements.

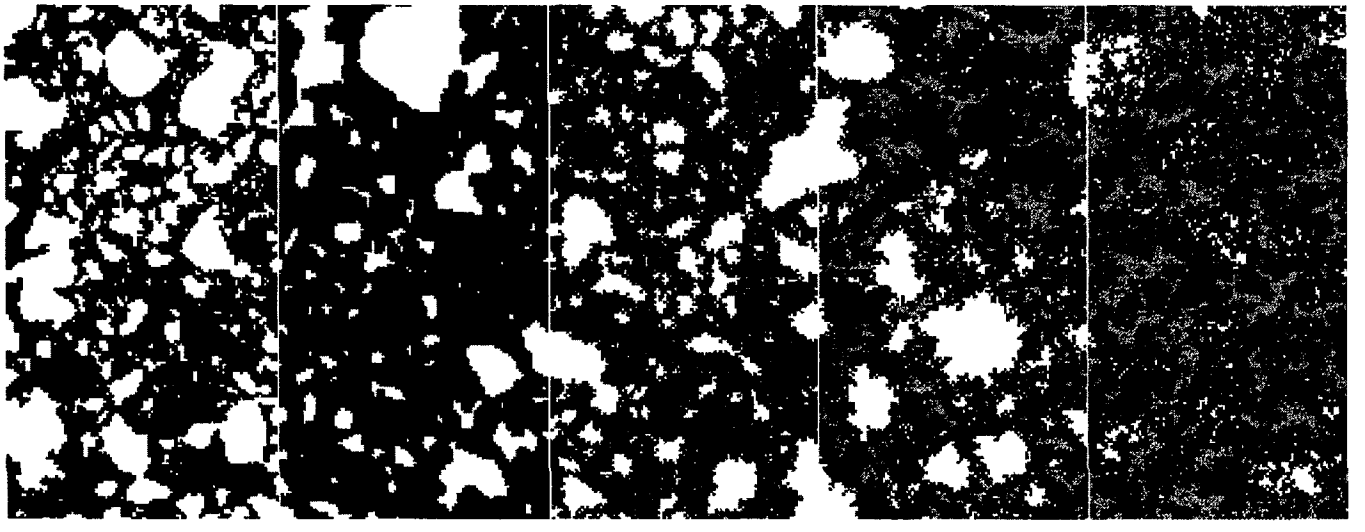

FIGURE 2 Illustration of steps in C_3S hydration microstructural model.

gray, calcium silicate hydrate gel is dark gray, and capillary porosity is black. The far left image shows an initial packing of cement particles in water, while the second image illustrates the identification of all C_3S sites (pixels) eligible for random dissolution, highlighted in gray. The middle image shows the system after dissolution, with many individual diffusing species having been generated and now undergoing reactions. The two rightmost images illustrate hydrated microstructures after 51 percent and 87 percent hydration, respectively.

To create a three-dimensional microstructure, digitized spherical particles following the particle size distribution (PSD) measured for the cement powder of interest are placed at random locations in a three-dimensional (3-D) digital image typically 100 or 200 pixels on a side. By selecting the number of particles placed, the user may control the water-to-cement (w/c) ratio of the cement paste. Each pixel element in the 3-D volume represents a volume of 1 μm^3, so that particles may range from 1 μm to about 40 μm in diameter, which covers most of the PSD range for a conventional cement. Periodic boundaries are used such that if a portion of a particle extends beyond the hydration volume boundaries, it is completed by protruding it through the opposite face of the cubic volume. During placement, particles can be flocculated or dispersed to provide a more realistic representation of an actual cement-water mixture (*12*). The cellular automaton algorithm is then used to create a microstructure at a desired degree of hydration.

Microstructure Model for Mortar or Concrete

Because of the large-scale range encompassed by the aggregates in a typical concrete, models that are solely digital-image-based quickly encounter severe memory limitations. A more practical approach is provided by the use of a continuum hard core–soft shell model to represent the concrete (*9,10*). Here, the aggregates are usually modeled as spheres, each characterized by a centroid (x,y,z) and a radius. Each aggregate is surrounded by a concentric shell, which represents the ITZ region. Thus, while the hard core aggregates may not overlap one another, the soft shell ITZ regions are free to overlap one another or partially overlap a hard core region. For spheres, these overlaps can be evaluated for any two particles based on a simple comparison of the centroid-to-centroid distance to the sum of the radii of the particles. Although the calculation is more complex for general ellipsoidal particles, computer models have been developed to examine the percolation or connectivity of the ITZ regions in ellipsoid-based systems of various aspect ratios as well (*13*).

For mortars, the typical computational volume used in the simulations is 1 cm^3, which requires on the order of 20,000 individual sand grains. For concrete, where a volume of 27 cm^3 is used, a simulation may require as many as 500,000 particles. The particles are placed from largest to smallest at random locations in the 3-D volume using periodic boundaries. The left side of Figure 3 shows a 2-D slice from a 3-D model for a typical mortar. A continuum burning algorithm (*9*) is used to assess the percolation of the ITZ regions for a given configuration of the model by determining whether a pathway through overlapping ITZs traverses the microstructure. Computationally, each particle whose ITZ contacts the top surface of the 3-D microstructure is marked, and this marking propagated (like the spread of a fire) to all additional particles whose ITZ regions partially overlap one or more of the initially marked particles. This algorithm is applied iteratively until all "connected" particles are marked. If the ITZ of any marked particle also contacts the bottom surface of the 3-D microstructure, a continuous pathway through the ITZ regions must exist. Additionally, digitization (3-D point sampling) is used to determine the volume fractions occupied by aggregates, ITZ cement paste, and bulk cement paste.

Computation of Diffusivity

The computer modeling techniques used to estimate the diffusivity of cement paste and concrete have been described in detail elsewhere (*4,10*). Here, we shall concentrate on the linkage of the two previously described microstructure models to develop an integrated multiscale model for the diffusivity of concrete or mortar as illustrated in

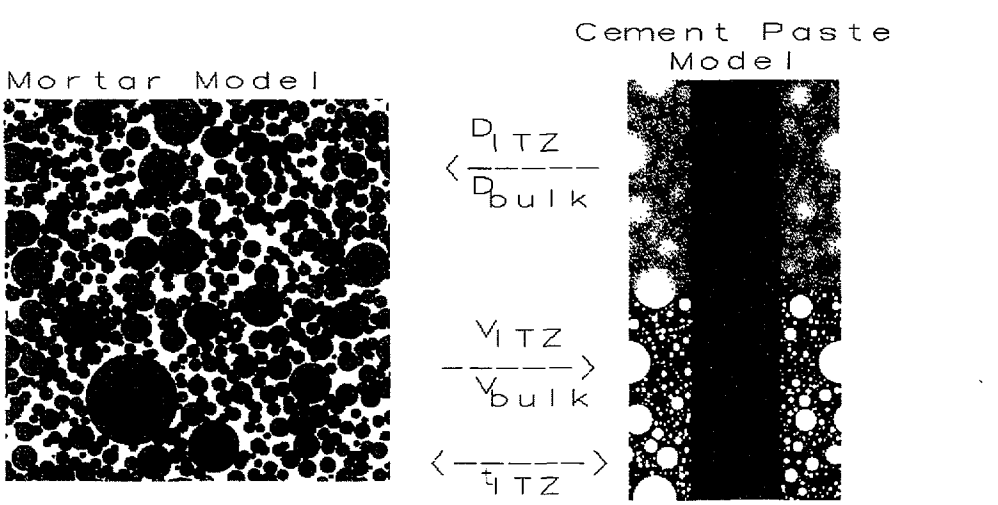

FIGURE 3 Linkages between microstructure models for mortar and cement paste for predicting diffusivity of mortar or concrete. Arrows indicate flow of information between models needed to compute diffusivity of mortar.

Figure 3. For the mortar model on the left side of Figure 3, aggregates are gray, ITZ regions are black, and bulk cement paste is white. In the cement paste images on the right side, cement particles are white, water-filled capillary porosity is black, and the single central rectangular-shaped aggregate is gray. In the hydrated microstructure on the top right, calcium hydroxide is dark gray and calcium silicate hydrate gel is light gray. To successfully represent the microstructure of a concrete and its component paste as shown in Figure 3, the following input parameters are necessary: (a) mixture proportions (aggregate content, w/c ratio, and air content), (b) the PSDs of the cement and aggregates, and (c) the degree of hydration (α) of the cement paste in the concrete at the time of interest.

To begin, the PSD of the cement particles is used to estimate the thickness of the interfacial zone regions (t_{ITZ}) present in the concrete. Simulation studies have shown that t_{ITZ} can be estimated as the median diameter of the cement particles on a mass basis (*14*). Thus, a typical value would be on the order of 20 μm. This ITZ thickness is input into the hard core–soft shell model of the mortar or concrete, as indicated in Figure 3, along with the aggregate content and the aggregate PSD (e.g., based on a sieve analysis). In the present work, the measured air contents of the mortar are incorporated into the model by increasing the aggregate content to represent the sum of the air and sand volume fractions. Thus, at present, we are *assuming* that the air voids follow a size distribution similar to that of the sand. However, if the air void size distribution has been quantified, the total inclusion size distribution can be easily modified to represent contributions of both the sand and air void sizes.

As described for the mortar microstructure model, a burning algorithm is executed to assess percolation and digitization used to determine the volume fractions of bulk and ITZ cement paste. These volume fractions (V_{ITZ} and V_{bulk}) are then input into the cement paste hydration microstructure model, as indicated by the arrow going from the mortar model to the cement paste model in Figure 3. The cement paste model uses a system containing a single aggregate particle to simulate the microstructure development in the ITZ and bulk paste regions (right side of Figure 3). The thickness of the aggregate particle in this system is adjusted to obtain the appropriate volume fractions of ITZ and bulk cement paste for the chosen value of t_{ITZ}.

The cement paste is hydrated until some desired overall degree of hydration is achieved. Then, point sampling is used to determine the variation in capillary porosity as a function of distance from the aggregate surface. Additionally, the average porosity in the ITZ and bulk paste regions can be computed. The following empirical equation (*4*) can be used to convert capillary porosity (ϕ) into a relative diffusivity (the ratio of the diffusivity of ions in the cement paste to their diffusivity in bulk water):

$$\frac{D}{D_0} = 0.001 + 0.07 * \phi^2 + 1.8 * H(\phi - 0.18) * (\phi - 0.18)^2 \qquad (1)$$

where all symbols are defined in the Notation section at the end of this paper. Thus, the ratio of the ITZ [D_{ITZ}/D_0 (ϕ_{ITZ})] to the bulk paste [$D_{bulk}/D_0(\phi_{bulk})$] relative diffusivity can be determined.

These diffusivity values are returned to the original mortar model as indicated by the arrow flowing from the cement paste model to the mortar model in Figure 3. Then, this ratio of ITZ to bulk cement paste diffusivity is used in a myopic random walker algorithm, implemented in the original hard core–soft shell representation of the concrete, to estimate the diffusivity of the original mortar or concrete microstructure relative to its bulk cement paste value (*10*). Typically, 10,000 walkers are placed at random locations in the bulk and ITZ cement paste (not in the aggregates). Each random walker maintains a record of its cumulative travel time, its starting location, and its current location. Each walker's steps are of a constant length in a random direction in 3-D space. The amount of time that elapses during a step depends on the starting and ending locations of the step (e.g., a step entirely within the ITZ paste takes less time than a step entirely within the bulk paste due to the higher relative diffusivity of the former). The walkers are not allowed to step into the aggregates or air voids, but their clock still advances when such an attempted step is made. Additionally, the probability of a walker being allowed to step from an ITZ region into a bulk paste region is biased by the ratio of its relative diffusivity in the two media (*15*). By dividing the distance traveled squared by the time elapsed after a large number of steps (e.g., 200,000), an estimate of the diffusivity of the walker in the composite media can be determined. By averaging this value over the 10,000 walkers and multiplying by the total cement paste (ITZ + bulk) volume fraction, an estimate of the relative diffusivity of the mortar or concrete (D_M/D_{bulk}) can be obtained. This value can be converted into an absolute diffusion coefficient for comparison against experimental data by multiplying it by the relative diffusivity of the bulk cement paste determined using Equation 1 and the diffusion coefficient of the ions of interest in bulk water [$D_M = (D_M/D_{bulk})(D_{bulk}/D_0)D_0$].

RESULTS

Few data sets in the literature provide all the necessary information for validating the multiscale model. However, a data set for a series of mortars of varying sand content was provided in Halamickova's recent master's thesis (*16*) and summarized in (*17*). Information is provided on the cement and aggregate PSDs, α of the mortars, and the diffusion coefficients measured for chloride ions using an accelerated electrochemical technique. Experiments were performed for two w/c ratios (0.4 and 0.5 by mass) and four different sand volume fractions (0, 35, 45, and 55 percent). The air contents, while not measured for each individual specimen, were assessed for both the neat cement pastes (1 percent) and mortars (8 percent).

Equation 1 can be directly applied for estimating the relative diffusivity of the neat cement paste samples. To do this, it is necessary to convert the degree of hydration values measured experimentally (*16*) to capillary porosity values, according to the following equation (*18*):

$$\phi = 1. - \frac{(1. + 1.31 * \alpha)}{\left(1. + 3.2 * \frac{w}{c}\right)} \qquad (2)$$

where the quantity 3.2 is the density of cement in graves per cubic centimeter and the quantity 1.31 represents the relative increase in solids volume due to the hydration reaction. To convert from relative to absolute diffusivities, a value of $2.0 * 10^{-9}$ m^2/sec at 25°C is used for the temperature-dependent diffusion coefficient of chloride ions in water (*19*).

Following the procedures outlined above, the mortars investigated experimentally (*16*) were modeled using the multiscale approach, assuming an ITZ thickness of 20 μm. The computed diffusivity values could then be directly compared to those measured experimentally (*16*). Figures 4 and 5 compare the experimental and model results for the two w/c ratios of 0.40 and 0.50. For the

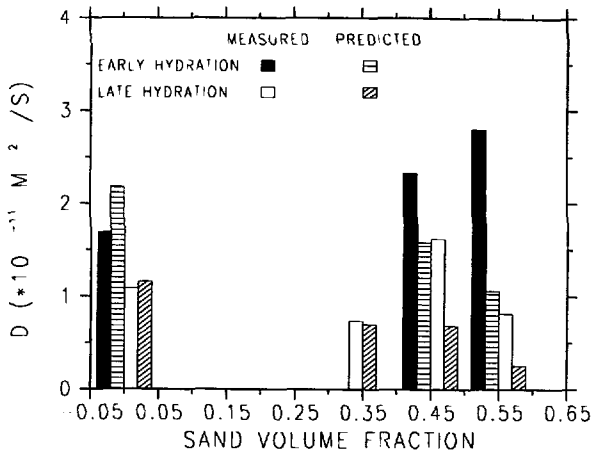

FIGURE 4 Comparison of experimental and model diffusion coefficients for *w/c* = 0.40.

pastes (0 percent sand), early hydration corresponds to 50 to 55 percent while late hydration is in the range of 55 to 60 percent. For the mortars, hydration is accelerated, with early hydration in the range of 50 to 60 percent and late hydration corresponding to 65 to 75 percent (*16*). The experimentally determined diffusivities are generally larger, but within a factor of 2 of the model results. Furthermore, in several cases, the model values are within 10 percent of the experimentally measured ones. Given the assumptions made concerning the air void distribution and so forth, this agreement seems reasonable.

CONCLUSIONS

Digital-image-based computer modeling of cement-based materials allows for both visualization of the ongoing microstructural development and the straightforward computation of physical properties. Here, two different scale microstructure models have been linked to provide a multiscale modeling of the diffusivity of mortar and concrete. Quantitative results, based on the analysis of digital images, are transferred between the two levels to allow an estimation of diffusivity based on the actual experimental details (PSDs, mixture proportions, and α). In this preliminary comparison, the agreement between experimental results and model predictions is quite good. The multiscale modeling approach presented here will allow the diffusivity of a mortar or concrete at an anticipated degree of hydration to be computed, thus providing the basis for rapid estimates for use in service-life prediction models and in durability design codes.

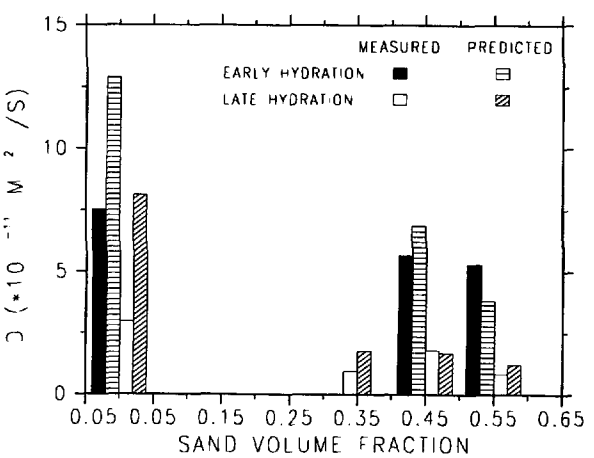

FIGURE 5 Comparison of experimental and model diffusion coefficients for *w/c* = 0.50.

NOTATION

α = degree of hydration,
ϕ = capillary porosity,
D = diffusivity,
$H(x)$ = Heaviside function = (1: $x \geq 0$; 0: otherwise),
t = thickness,
V = volume fraction,
w/c = water-to-cement ratio,
bulk = bulk cement paste,
0 = bulk solution,
ITZ = interfacial transition zone cement paste, and
M = mortar.

REFERENCES

1. Bentz, D. P., and E. J. Garboczi. Digital-Image-Based Computer Modeling of Cement-Based Materials. In *Digital Image Processing: Techniques and Applications in Civil Engineering* (J. D. Frost and J. R. Wright, eds.). ASCE, New York, 1993, pp. 44–51.
2. Wolfram, S. *Theory and Applications of Cellular Automata*. World Scientific, Singapore, 1986.
3. Bentz, D. P., P. V. Coveney, E. J. Garboczi, M. F. Kleyn, and P. E. Stutzman. Cellular Automaton Simulations of Cement Hydration and Microstructure Development. *Modeling and Simulation in Materials Science and Engineering*, Vol. 2 No. 4, 1994, pp. 783–808.
4. Garboczi, E. J., and D. P. Bentz. Computer Simulation of the Diffusivity of Cement-Based Materials. *Journal of Materials Science*, Vol. 27, 1992, pp. 2083–2092.
5. Garboczi, E. J., and A. R. Day. An Algorithm for Computing the Effective Linear Elastic Properties of Heterogeneous Materials: Three-Dimensional Results for Composites with Equal Phase Poisson Ratios. *Journal of Mechanics and Physics of Solids*, Vol. 43, No. 9, 1995, pp. 1349–1362.
6. Bentz, D. P., D. A. Quenard, V. Baroghel-Bouny, E. J. Garboczi, and H. M. Jennings. Modeling Drying Shrinkage of Cement Paste and Mortar: Pt 1. Structural Models from Nanometers to Millimeters. *Materials and Structures*, Vol. 28, 1995, pp. 450–458.
7. Bentz, D. P., E. J. Garboczi, H. M. Jennings, and D. A. Quenard. Multi-Scale Digital-Image-Based Modeling of Cement-Based Materials. In *Microstructure of Cement-Based Systems/Bonding and Interfaces in Cementitious Materials* (S. Diamond et al. eds.). Materials Research Society, Pittsburgh, Pa., 1995, pp. 33–42.
8. Bentz, D. P., and E. J. Garboczi. Guide to Using HYDRA3D: A Three-Dimensional Digital-Image-Based Cement Microstructure Model. NISTIR 4746. U.S. Department of Commerce, 1992.
9. Winslow, D. N., M. D. Cohen, D. P. Bentz, K. A. Snyder, and E. J. Garboczi. Percolation and Pore Structure in Mortars and Concrete. *Cement and Concrete Research*, Vol. 24 No. 1, 1995, pp. 25–37.
10. Garboczi, E. J., L. M. Schwartz, and D. P. Bentz. Modeling the Influence of the Interfacial Zone on the Conductivity and Diffusivity of Mortar. *Journal of Advanced Cement-Based Materials*, Vol. 2, 1995, pp. 169–181.
11. Bentz, D. P., and P. E. Stutzman. SEM Analysis and Computer Modeling of Hydration of Portland Cement Particles. In *Petrography of Cementitious Materials* (S. M. Dehayes and D. Stark, eds.). ASTM, Philadelphia, Pa., 1994, pp. 60–73.

12. Bentz, D. P., E. J. Garboczi, and N. S. Martys. Application of Digital-Image-Based Models to Microstructure, Transport Properties, and Degradation of Cement-Based Materials. In *Computer Modeling of Microstructure and Its Potential Application to Transport Properties* (H. M. Jennings, ed.). RILEM, Paris, France, 1995, pp. 167–186.
13. Bentz, D. P., J. T. G. Hwang, C. Hagwood, E. J. Garboczi, K. A. Snyder, N. Buenfeld, and K. L. Scrivener. Interfacial Zone Percolation in Concrete: Effects of Interfacial Zone Thickness and Aggregate Shape. In *Microstructure of Cement-Based Systems/Bonding and Interfaces in Cementitious Materials* (S. Diamond et al. eds.). Materials Research Society, Pittsburgh, Pa., 1995, pp. 437–442.
14. Bentz, D. P., E. Schlangen, and E. J. Garboczi. Computer Simulation of Interfacial Zone Microstructure and Its Effect on the Properties of Cement-Based Composites. In *Materials Science of Concrete IV* (J. P. Skalny and S. Mindess, eds.). American Ceramic Society, Westerville, Ohio, 1994, pp. 155–199.
15. Schwartz, L. M., E. J. Garboczi, and D. P. Bentz. Interfacial Transport in Porous Media: Application to D.C. Electrical Conductivity of Mortars. *Journal of Applied Physics*, Vol. 78, No. 10, 1995, pp. 5898–5908.
16. Halamickova, P. *The Influence of Sand Content on the Microstructure Development and Transport Properties of Mortars*. M.S. thesis. University of Toronto, 1993.
17. Halamickova, P., R. J. Detwiler, D. P. Bentz, and E. J. Garboczi. Water Permeability and Chloride Ion Diffusion in Portland Cement Mortars: Relationship to Sand Content and Critical Pore Diameter. *Cement and Concrete Research*, Vol. 24 No. 4, 1995, pp. 790–802.
18. Bentz, D. P., and E. J. Garboczi. Percolation of Phases in a Three-Dimensional Cement Paste Microstructural Model. *Cement and Concrete Research*, Vol. 21 No. 2, 1991, pp. 325–344.
19. Mills, R., and V. M. M. Lobo. *Self-Diffusion in Electrolyte Solutions*. Elsevier Press, Amsterdam, Netherlands, 1989, p. 317.

Publication of this paper sponsored by Committee on Soil and Rock Properties.